Adv. Polar Upper Atmos. Res., **14**, 221–232, 2000

Quantification of neutral turbulence in the mesosphere and lower thermosphere using EISCAT and ESR

C. M. Hall

Tromsø Geophysical Observatory, University of Tromsø, 9037 Tromsø, Norway

Abstract: Incoherent scatter radar have traditionally determined four ionospheric parameters: electron density, ion temperature, electron temperature and ion velocity. From these it is possible to derive further atmospheric parameters such as electric field. In order to detect neutral turbulence, a radar's wavelength must be somewhat longer than that used for incoherent scatter, such that scattering arises from turbulent "eddies" instead of plasma waves. However, by using a suitably high height and time resolution, it is possible to investigate turbulence from the velocity information alone. This review will describe the methods hitherto used to quantify neutral turbulence in this way and using the EISCAT incoherent scatter systems on the Norwegian mainland and Svalbard.

1. Introduction

In this review, a treatise in turbulent theory would be out of place; however, a qualitative introduction allows us to introduce some nomenclature. Let us suppose one was to measure velocity of a neutral turbulent flow with high precision and temporal resolution. The resulting time series would conceivably be characterized by a background motion with chaotic fluctuations superimposed upon it. Forming the power spectrum of the fluctuation component would result in the turbulent energy spectrum, and this might well display the power law dependence often associated with the work of Kolmogorov (1941). A schematic representation of this kind of spectrum is shown in Fig. 1. Here turbulence in the atmosphere is envisaged: at small wavenumbers corresponding to frequencies smaller than the Brunt-Väisälä frequency, buoyant motion dominates (the buoyancy subrange); beyond this, between the outer and inner scales (L_B and l_0 respectively) inertial forces dominate and energy is transferred from larger to smaller scales without loss (the inertial subrange). At the famous Kolmogorov microscale, η, turbulent and molecular diffusion are equal, and it is common to assume $\eta \sim l_0/10$ (*e.g.* Heisenberg, 1948). Finally, at scales smaller than the inner scale, the spectral slope steepens and kinetic energy is transformed into heat as viscosity damps the eddy motion (the viscous subrange). The structures in refractive index that form in the inertial subrange scatter radio waves and in this way a radar satisfying the Bragg condition between L_B and l_0 will receive a signal whose strength depends on the turbulent intensity. For further reading on turbulence theory, Tennekes and Lumley (1972) is recommended; Kundu (1980) explains application to atmospheric physics, while Hocking (1987) is a source of references for application of the theory to radar observations.

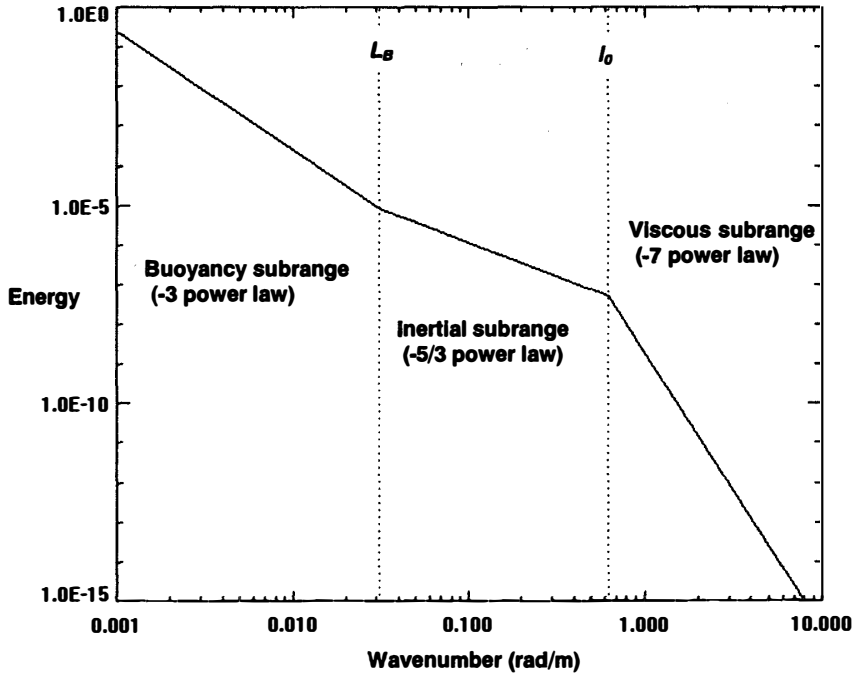

Fig. 1. Schematic energy spectrum for neutral velocity fluctuations. The buoyancy subrange (driven by progressively shorter period gravity waves), characterised by a –3 power law is on the left. The inertial subrange, in the centre is characterised by a –5/3 power law dependence when the turbulence is homogeneous and isotropic. To the right is the viscous-dissipative subrange, characterised by a –7 power law dependence. L_B denotes the "outer scale"; l_0 denotes the "inner scale".

A typical size for L_B is 200 m, and for l_0 a few metres depending on the strength of turbulence (l_0 might typically be 10 m in moderate turbulence in the mesosphere). Thus radars such as EISCAT VHF (Baron, 1984), with a 1/4-wavelength of only 30 cm are unlikely to receive echoes from inertial subrange eddies. The viscous subrange should exhibit a –7 power law dependence on wavenumber according to Heisenberg (1948), although the exactness is addressed by Batchelor (1953, Chapter VII). For this reason, incoherent scatter usually dominates the received signal in this regime. Significant coherent signals received at these wavelengths (*e.g.* Ecklund and Balsley, 1981) and dubbed Polar Mesospheric Summer Echoes (PMSE) by Hoppe *et al.* (1988) may well be related to neutral turbulence but are rather caused by very high Schmidt number (Hill and Clifford, 1978) tracers (Kelley and Farley, 1987) such as macro-ions (Hall, 1990) and are not representative of the true neutral-air density structures. Thus, it would appear that the EISCAT radars are little suited to investigation of turbulence.

In the mesosphere, where the incoherent scatter spectrum is dominated by ion-neutral collisions, the spectral form is somewhat constant (Mathews, 1966). The incoherent scatter spectra remain Lorentzian in form although the characteristic width may change due to ion-mass, temperature or the presence of negative ions. This limits their use since ionospheric parameters cannot be determined unambiguously. In fact, the only parameter that may be determined with any degree of confidence is the line-of-sight velocity. Since the spectra are indeed collision dominated, it is reasonable to assume that the line-of-sight ion velocity is also representative of the neutral velocity, at least below

90 km. At greater heights, the ion motion departs steadily more from that of the neutrals, particularly in the presence of an electric field (*e.g.* Fujii *et al.*, 1998). However, by simultaneously measuring the ion vector velocity in the F-region, where the ions are effectively decoupled from the neutrals, it is possible for systems such as EISCAT to estimate the electric field. Assuming the electric field may be mapped down the geomagnetic field, this information may be combined with ion velocity measurements in the lower thermosphere to estimate the neutral motion.

2. Early work—first generation approach

Prior to 1996, regular turbulence measurements in northern Norway were largely performed *in situ* using soundings from the rocket launching facility on Andøya (69°N, 16°E), recently summarised by Hall *et al.* (1997). One notable exception to this was the work of Schlegel *et al.* (1978) who used the (then) University of Tromsø MF-radar in an exploratory way.

The European Incoherent Scatter radar facility (EISCAT) (69°N, 19°E) began regular observations in the early 80's (Baron, 1984). Since around the discovery of PMSE by Hoppe *et al.* (1988), a particular experiment, "CP-6" (Turunen, 1986) has been performed regularly on the VHF system (224 MHz), and vertical velocities have been obtained with an almost complete year-round coverage. It became apparent that these vertical velocity measurements, offering profiles from 70 to 90 km every kilometre and every 5 min for periods up to 36 hours, could be used to derive fluctuations in kinetic energy. A kind of longitudinal structure function was derived:

$$D_{rr}^2 = \overline{(w(z) - w(z+\Delta z))^2}, \tag{1}$$

in which w is the vertical velocity component and z is height (Blamont, 1963). The reason that this "structure function" cannot be directly used to estimate the turbulent energy dissipation rate, ε, is that the height increment, Δz cannot be guaranteed smaller than the largest eddies. In fact, one might expect $L_B \approx 200$ m in the mesosphere (*e.g.* Blix *et al.*, 1990) as opposed to the 1 km offered by the CP-6 experiment. Nevertheless, the method produced results that were not unlike other ground-based derivations of ε; the method was published by Hall (1997) and a typical profile of kinetic energy dissipation rate, e_g derived from:

$$e_g = D_{rr}^3 / \Delta z, \tag{2}$$

is shown in Fig. 2. By utilising all available CP-6 experiments, it has been possible to arrive at the annual variation, shown in Fig. 3. It is in this figure that one may see that e_g does not reproduce the behaviour anticipated of ε: a maximum in turbulent energy dissipation is expected in the lower thermosphere in summer, with little or no energy dissipation in the mesosphere below (Hocking, 1987; Lübken 1997). The method of Hall (1997) was very simplistic, but represented a pioneering attempt to use incoherent scatter radar data in a novel way; the results, particularly for the winter months were remarkably believable and the study gave impetus for further work.

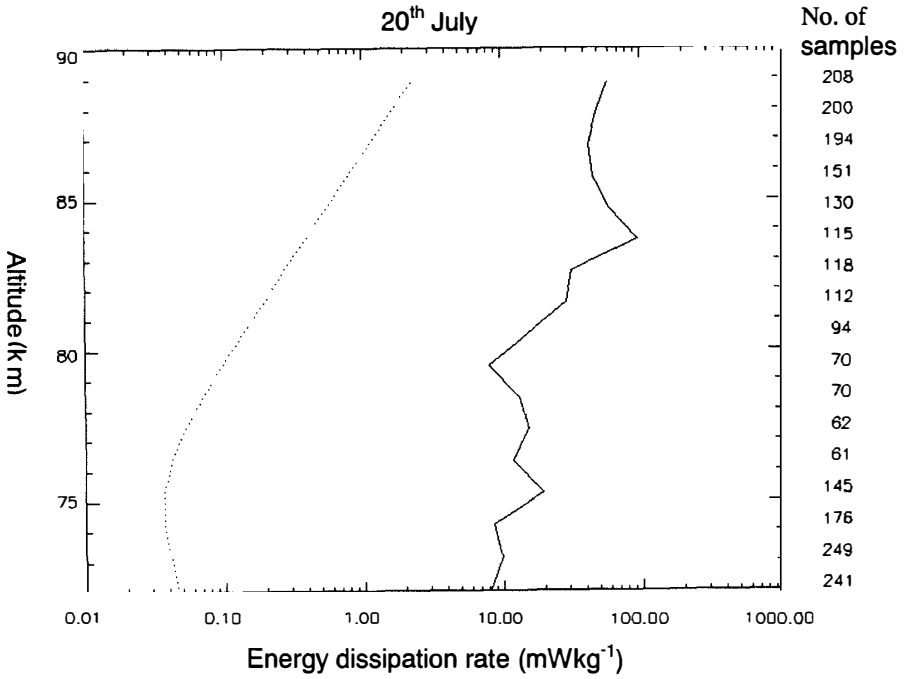

Fig. 2. Kinetic energy dissipation rate profile determined by EISCAT VHF vertical velocity measurements for 20th July 1993. The dotted line shows the minimum turbulent energy dissipation rate supported by the atmosphere (i.e. for if inner and outer scales coincided). The right hand axis annotation indicates the numbers of 5-min profile values that have contributed to each data point.

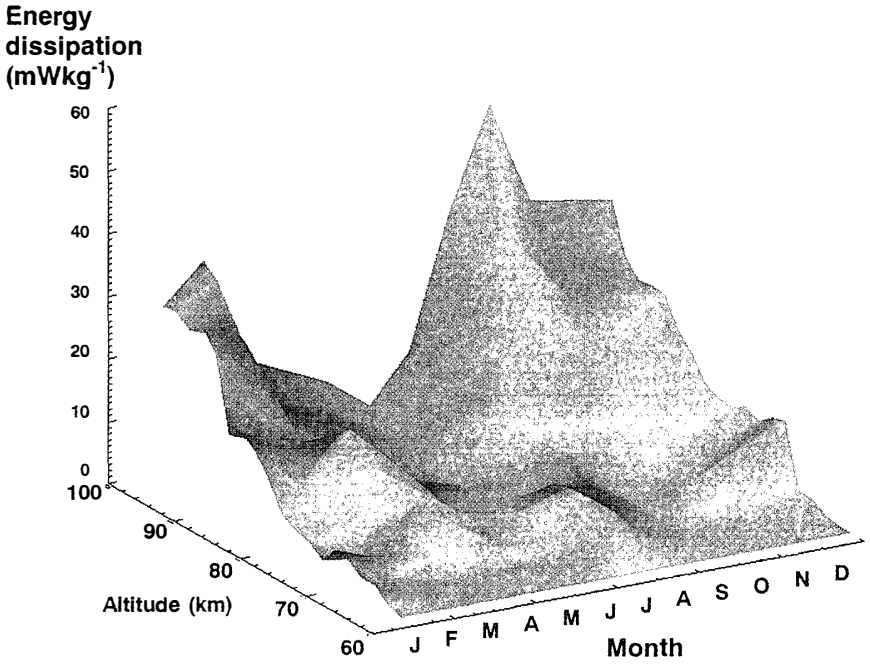

Fig. 3. Kinetic energy dissipation rate profile determined by EISCAT VHF vertical velocity measurements for all CP-6 experiments as a function of season and altitude.

3. Second generation approaches

The high signal-to-noise-ratio returns from PMSE were used by Hoppe and Fritts (1995) to determine vertical velocity to rather higher precision than usual. In the companion paper, Fritts and Hoppe (1995) addressed the spectra of these vertical velocity variations and indicated how the resulting characteristic vertical wavenumbers, m_* a related to the total wave energy E_0 and the buoyancy frequency N:

$$E_0 = \frac{N^2}{10\, m_*^2}. \tag{3}$$

Fritts and Van Zandt (1993) demonstrate how m_* may be related to an upper limit for ε:

$$\varepsilon \approx \frac{NE_0}{18\, m_*}\left(\frac{1}{H} - \frac{3}{2H_E}\right), \tag{4}$$

where H and H_E are the density and energy scale heights respectively and $H_E = 2.3\ H$.

We shall refer to this "upper limit for turbulent energy dissipation rate" many times and thus denote it by ε'. By using large numbers of profiles to compensate for the lower signal-to-noise-ratios, Hall and Hoppe (1997) determined m_* from CP-6 incoherent scatter measurements, and were thus able to estimate ε'. The disadvantage of this method is that a height profile of vertical velocities yields only one characteristic vertical wavenumber, characteristic of the height range of the measurement. Furthermore, since any given profile does not necessarily have good data at every radar range gate, m_* applies to the average height, and this may not be the centre of the measurement interval. In addition, since the data points in each profile may be irregularly spaced (due to missing data) Hall and Hoppe (1997) used the Lomb-Scargle method of spectral analysis. This method yields characteristic wavenumbers and associated confidence levels, which, in turn facilitates automatic processing of large numbers of profiles and provides a rejection mechanism for doubtful (low confidence) results. These caveats must be remembered when averaging data and comparing with other methods. A typical vertical wavenumber spectrum is shown in Fig. 4. Employing the method for as much CP-6 data as was available at that time, Hall and Hoppe (1998) were able to investigate the seasonal variation of ε'. An example of seasonal variation of ε' using the m_* method is shown in Fig. 5, which clearly shows the expected semi-annual variation.

While seasonal and longer-term trends are important, Hall (1998) examined the tidal response of the kinetic energy. Clear modulation of the energy by the combined tides was observed, but the effect was seen to be considerably greater around the equinox months when the overall upper mesosphere energy dissipation rates are lowest. The relative importance of the tidal modes as functions of height and season can be seen in Fig. 6. Here, the complete set of CP-6 measurements have been sorted according to season, and then, for each of spring, summer, autumn and winter, day-averages were formed.

Several facilities for upper atmosphere research are located in northern Norway: the EISCAT UHF and VHF radars share a site with the joint Universities of Tromsø, Saskatchewan and Nagoya MF radar; the Andøya Rocket range lies some 130 km to the west together with mutually supporting ground-based instruments. Comparison of results from completely independent methods is relatively straightforward. Hall *et al.* (1999a)

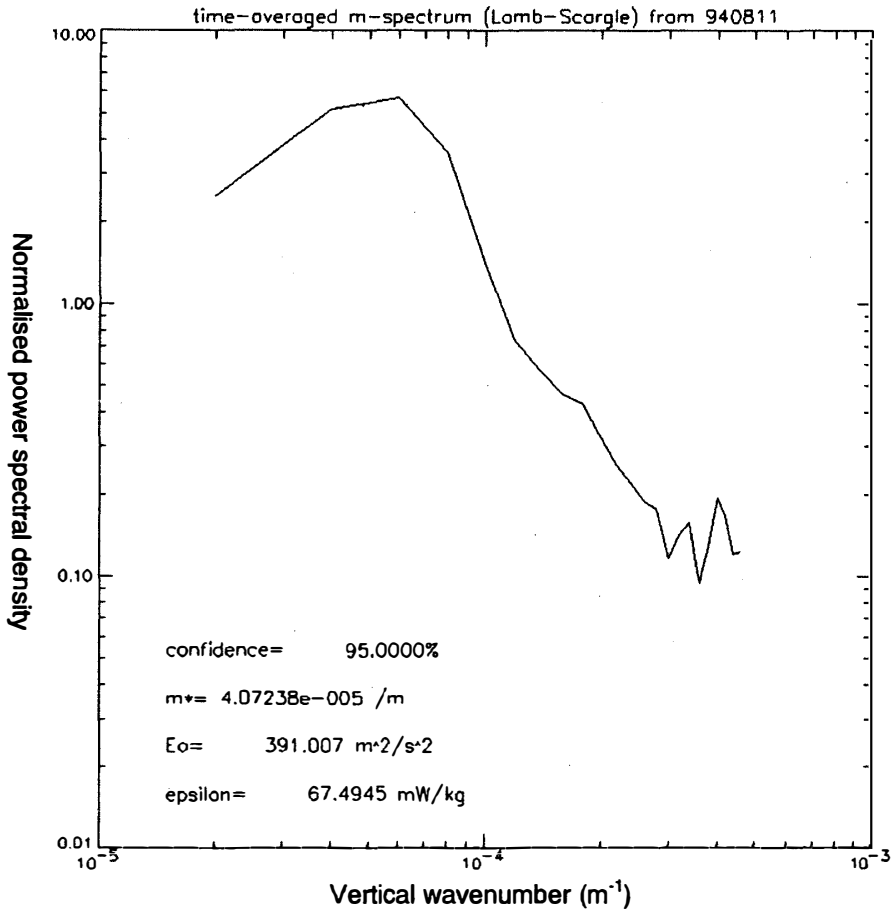

Fig 4. Example of vertical wavenumber spectrum obtained using EISCAT VHF. The characteristic vertical wavenumber has been identified along with the total wave energy and upper limit for turbulent energy dissipation rate.

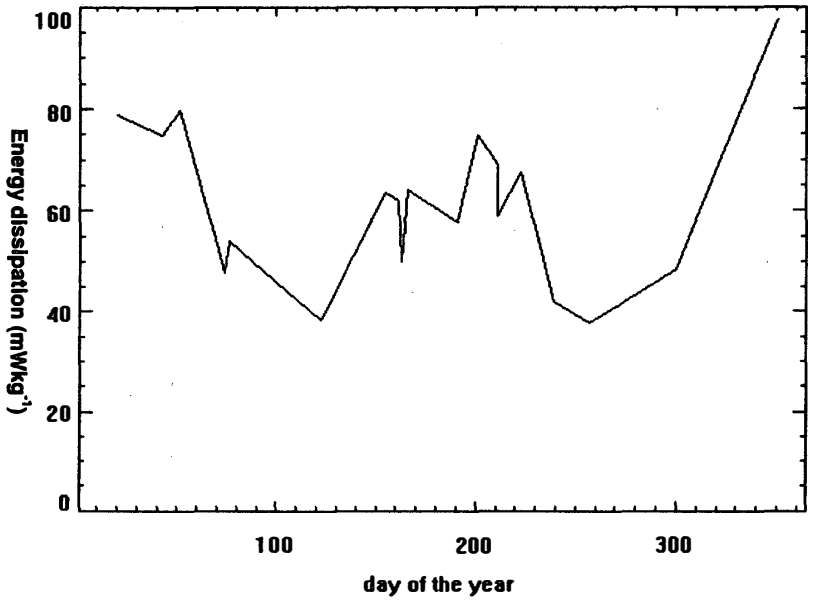

Fig. 5. Upper limits for energy dissipation rate using characteristic vertical wavenumbers obtained from EISCAT VHF—the seasonal variation for 1997 is shown (Hall and Hoppe, 1998).

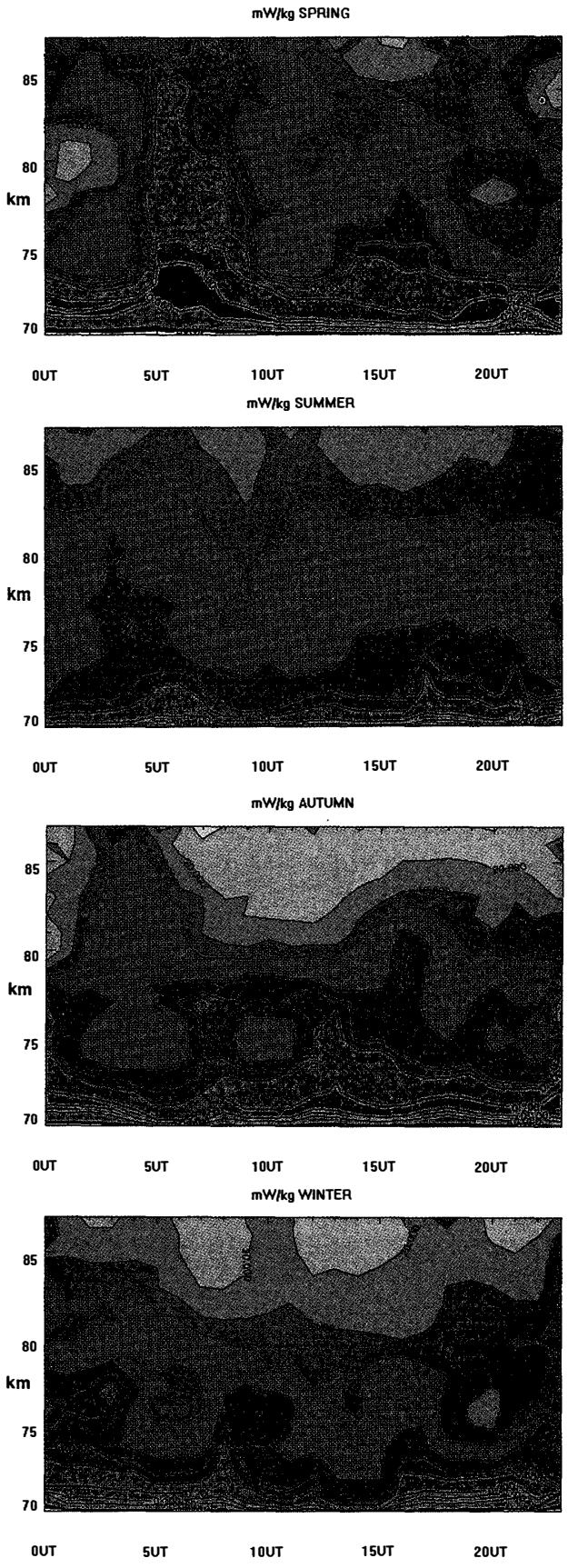

Fig. 6. Kinetic energy dissipation rate (method of Hall, 1997) as a function of time of day, height and season, in order to illustrate tidal dependence (Hall, 1998). Contours are in $mWkg^{-1}$.

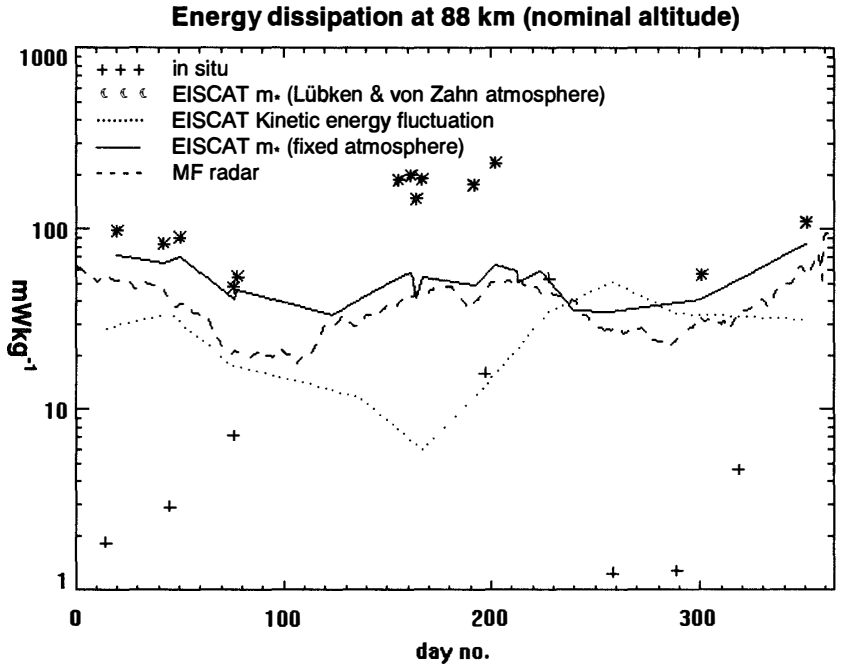

Fig. 7. Seasonal variation of energy dissipation rate (see text for explanation of the different definitions. The EISCAT m_* method has been performed for two different model atmospheres, to illustrate the sensitivity to scale height and buoyancy frequency (Hall and Hoppe, 1998).

have reviewed some contemporary methods of estimating ε (or ε' in some cases), and attempted to highlight the main assumptions inherent in each method. Figure 7 shows a comparison of ε and ε' estimates from both *in situ* and ground based observations including those already discussed. Here, the *in situ* measurements are fully described in the references found in Hall *et al.* (1997); the MF radar is described in Hall *et al.* (1998). One can see from Fig. 7 that there is general agreement between the radar-based methods. The simplistic assumptions inherent in the kinetic energy variation are presumably inappropriate for approximation to ε in the summer months; the reason is unknown. The *in situ* measurements indicate radically lower turbulent intensities in winter; this may be due to the other instruments measuring ε'. Again, the exact reasons for such differences remain an unsolved problem in this field.

4. Recent studies

The installation of the EISCAT Svalbard Radar (ESR) (Wannberg *et al.*, 1997) has opened up the possibilities for studies similar to those described above, but at even higher (80°N) latitude. Being of a higher operating frequency (500 MHz), ESR is less suited to *D*-region studies than EISCAT VHF. Exploratory *D*-region work was performed by Hall *et al.* (1999b) sweeping the ESR antenna between west and northwest at low elevation and later combining the electron density information with that from an ionosonde and a rocket-borne ion probe. If the antenna is pointed at low elevation such that primarily the horizontal wind is measured, Doppler shifts are large and the corresponding uncertainty minimised. Indeed, since the horizontal wind almost invariably

dominates over the vertical component, any off-zenith antenna position is likely to "pick up" the horizontal component. Hall and Aso (1999) measured the zonal wind in the mesosphere and lower thermosphere over Svalbard using the same low elevation method but with fixed azimuth. They argued that collision frequencies were sufficiently high that the horizontal ion wind, converted from the line-of-sight observation by simple geometry, was a good approximation to the neutral wind. Subsequently they were able to estimate buoyancy subrange spectral slopes.

Danilov *et al.* (1979) have documented a series of *in situ* measurements of turbopause height above Heiss Island (80°N, 60°E) and reported a dependence on geomagnetic activity. Due to the nature of the publication, no explanation was offered as to the underlying mechanism. One possible explanation for this phenomenon is that when a strong electric field drives the ions near or at the turbopause, ion-drag (*e.g.* Fujii *et al.*, 1998) is sufficient to generate (or enhance existing) dynamic instability in the neutral gas. The work of Hall and Aso (1999) illustrates the potential for using ESR for validation of this theory. One might envisage deriving the stability metrics:

$$Ri = \frac{\omega_B^2}{\left(\frac{dU}{dz}\right)^2}, \tag{5}$$

where Ri is the gradient Richardson number, ω_B is the Brunt-Väisälä frequency in rad s^{-1}, U is the horizontal neutral wind and z is height, and an analogy to the Reynolds Number:

$$\aleph \equiv \left| \frac{(\text{ion drag induced neutral wind}) \cdot L_B}{\nu} \right|, \tag{6}$$

where L_B is the turbulent outer scale and ν is the kinematic viscosity; $\aleph$ is an analogy to the Reynolds Number, but indicating the relative importance of ion-drag induced neutral dynamics over kinematic viscosity. The gradient Richardson Number is a classic indicator of atmospheric instability. When the second metric, $\aleph$ is less than unity, any neutral dynamics induced by ion-drag will tend to be damped out by viscous drag. Thus when $\aleph > 1$ and $Ri < 0.25$ (*e.g.* Weinstock, 1978) and the wind shear term in (5) is caused by ion-drag, it might be anticipated that electrodynamic driving of the neutral air will cause turbulence to occur. Hall and Aso (hitherto private communication, 1999) were able to estimate **E** by swinging the beam alternately west and south and determining the horizontal vector ion velocity in the *F*-region, and thus having estimated the *E*-region neutral wind (using Fujii *et al.*, 1998) could derive (5) and (6). The preliminary results are summarised in Fig 8, which shows the condition $\aleph > 1$ and $Ri < 0.25$ (actually $(\aleph - 1) \times (Ri - 0.25)$) as a function of height averaged over the period of measurement (24h starting at 18UT on 17th March 1999). It can be seen that generation of neutral-air turbulence was possible around 104 km. This work should be regarded as a pilot study, however: many assumptions are inherent (*e.g.* homogeneity and stationarity of the *F*-region ion-wind field) and models employed (*e.g.* L_B was taken to be 200 m for the purposes of Fig. 8). Current work involves using EISCAT UHF monostatic and tristatic derived electric, ion velocity, and neutral velocity fields to make similar tests that will subsequently be compared with turbulent intensity estimates obtained using the co-located MF radar (hitherto S. Nozawa, private communication, 1999).

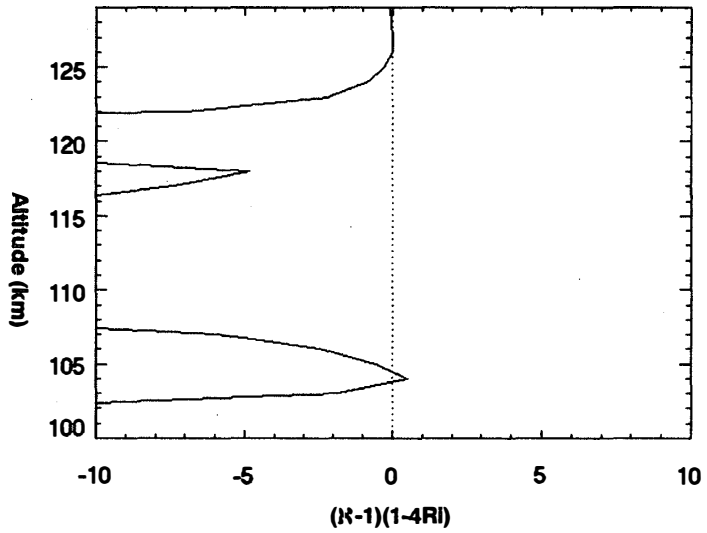

Fig. 8. Condition for ion-drag induced neutral air turbulence. When the line exceeds zero, the electrodynamics analogy to the Reynolds Number >1 and the gradient Richardson Number <0.25. See text for further explanation.

5. Summary

Incoherent scatter radars such as the EISCAT UHF, VHF and ESR systems are not normally thought of as instruments for measuring atmospheric turbulence. This is because the radio wavelengths they operate at are far smaller than the turbulent "eddies" present in the atmosphere. By making velocity measurements at sufficiently fine scales (either temporal or spatial), however, it is indeed possible to make estimates of turbulent intensity, although a number of assumptions are inherent. In particular, the velocity measured is an average for the entire scattering volume, which is almost certainly larger than the largest eddies. All ground-based and the majority of *in situ* methods of determining turbulent intensity make assumptions and approximations, particularly as described by Hall *et al.* (1999a) and Hocking (1999). One way of using such results is to avoid examining the absolute values of say, ε, since these are often affected by constants of proportionality with disputed values; rather, use the ground-based observations to look for variability and trends. Ground-based monitoring of turbulent intensity profiles remains the most cost-effective means of studying an important factor in mass and momentum transport and energy deposition in the upper atmosphere.

Acknowledgments

EISCAT is an International Association supported by Finland (SA), France (CNRS), the Federal Republic of Germany (MPG), Japan (NIPR), Norway (NFR), Sweden (NFR) and the United Kingdom (PPARC).

The editor thanks the referees for their help in evaluating this paper.

References

Baron, M. (1984): The EISCAT facility. J. Atmos. Terr. Phys., **46**, 469–472.

Batchelor, G.K. (1953): The theory of homogeneous turbulence. Cambridge, Cambridge University Press, 197 p.

Blamont, J.-E. (1963): Turbulence in atmospheric motions between 90 and 130 km of altitude. Planet. Space Sci., **10**, 89–101.

Blix, T.A., Thrane, E.V. and Andreassen, Ø. (1990): In situ measurements of the fine-scale structure and turbulence in the mesosphere and lower thermosphere by means of electrostatic positive ion probes. J. Geophys. Res., **95**, 5533–5548.

Danilov, A.D., Kalgin, U.A. and Pokhunov, A.A. (1979): Variation of the mesopause level in polar regions. Space Res., XIX, **83**, 173–176.

Ecklund, W.L. and Balsley, B.B. (1981): Long-term observations of the arctic mesosphere with the MST radar at Poker Flat, Alaska. J. Geophys. Res., **86**, 7775–7780.

Fritts, D.C. and Van Zandt, T.E. (1993): Spectral estimates of gravity wave energy and momentum fluxes. Part 1: Energy dissipation, acceleration and constraints. J. Atmos. Sci., **50**, 3685–3694.

Fritts, D.C. and Hoppe, U.-P. (1995): High-resolution measurements of vertical velocity with the European incoherent scatter VHF radar 2. Spectral observations and model comparisons. J. Geophys. Res., **100**, 16827–16838.

Fujii, R., Nozawa, S., Buchart, S.C., Matuura, N. and Brekke, A. (1998): The motion of ions in the auroral ionosphere. J. Geophys. Res., **103**, 20685–20695.

Hall, C. (1990): Modification of the energy-wavenumber spectrum for heavy proton hydrates as tracers for isotropic turbulence at the summer mesopause. J. Geophys. Res., **95**, 5549–5556.

Hall, C.M. (1997): Kilometer scale kinetic energy perturbations in the mesosphere derived from EISCAT velocity data. Radio Sci., **32**, 93–101.

Hall, C.M. (1998): Tidal signatures in mesospheric kinetic energy dissipation rates determined by EISCAT. Geophys. Res. Lett., **25**, 1941–1944.

Hall, C.M. and Aso, T. (1999): T. Mesospheric velocities and buoyancy subrange spectral slopes determined over Svalbard by ESR. Geophys. Res. Lett., **26**, 1685–1688.

Hall, C.M. and Hoppe, U.-P. (1997): Characteristic vertical wavenumbers for the polar mesosphere. Geophys. Res. Lett., **24**, 837–840.

Hall, C.M. and Hoppe, U.-P. (1998): Estimates of turbulent energy dissipation rates from determinations of characteristic vertical wavenumbers by EISCAT. Geophys. Res. Lett., **25**, 4075–4078.

Hall, C.M., Blix, T.A., Thrane, E.V. and Lübken, F.-J. (1997): Seasonal variation of mesospheric turbulent kinetic energy dissipation rates at 69°N. Proc.13th ESA symposium on European Rocket and Balloon Programmes and Related Research, 505–509.

Hall, C.M., Meek, C.E. and Manson, A.H. (1998): Turbulent energy dissipation rates from the University of Tromsø/University of Saskatchewan MF radar. J. Atmos. Solar Terr. Phys, **60**, 437–440.

Hall, C.M., Hoppe, U.-P., Blix, T.A., Thrane, E.V., Manson A.H. and Meek, C.E. (1999a): Seasonal variation of turbulent energy dissipation rates in the polar mesosphere: a comparison of methods. Earth Planet. Space, **51**, 515–524.

Hall, C.M., Van Eyken, A.P. and Svenes, K. (1999b): Plasma density over Svalbard during the ISBJØRN campaign. in press Annales. Geophysicae.

Heisenberg, W. (1948): Zur statistischen theorie der turbulenz. Z. Phys., **124**, 628–657 (in German).

Hill, R.J. and Clifford, S.F. (1978): Modified spectrum of atmospheric temperature fluctuations and its application to optical propagation. J. Opt. Soc. Am., **68**, 892–899.

Hocking, W.K. (1987): Turbulence in the region 80–120 km. Adv. Space Res., **7**, (10)171–(10)181.

Hocking, W.K. (1999): The dynamical parameters of turbulence theory as they apply to middle atmosphere studies. Earth Plant. Space, **51**, 525–541.

Hoppe, U.-P. and Fritts, D.C. (1995): High-resolution measurements of vertical velocity with the European incoherent scatter VHF radar 1. Motion field characteristics and measurement biases. J. Geophys. Res., **100**, 16813–16825.

Hoppe, U.-P., Hall, C. and Röttger, J. (1988): First observations of summer polar mesospheric backscatter

with a 224 MHz radar. Geophys. Res. Lett., **15**, 28–31.
Kelley, M.C. and Farley, D.T. (1987): The effect of cluster ions on anomalous VHF backscatter from the summer polar mesosphere. Geophys. Res. Lett., **14**, 1031–1034.
Kolmogorov, A.N. (1941): The local structure of turbulence in incompressible viscous fluid for very large Reynolds' numbers. C.R. Acad. Sci., U.R.S.S., **30**, 301–305.
Kundu, P.K. (1990): Fluid Mechanics. San Diego, Academic Press, 638 p.
Lübken, F.-J. (1997): Seasonal variation of turbulent energy dissipation rates at high latitudes as determined by in situ measurements of neutral density fluctuations. J. Geophys. Res., **102**, 13441–13456.
Mathews, J.D. (1966): Incoherent scatter radar probing of the 60–100 km atmosphere and ionosphere. IEEE Trans. Geo. Rem. Sens. **GE-24**, 765–776.
Schlegel, K., Brekke, A. and Haug, A. (1978): Some characteristics of the quiet polar D-region and mesosphere obtained with the partial reflection method. J. Atmos. Terr. Phys., **40**, 205–213.
Tennekes, H. and Lumley, J.L. (1972): A First Course in Turbulence. Massachusetts, MIT, 300 p.
Turunen, T. (1986): GEN-SYSTEM—a new experimental philosophy for EISCAT radars. J. Atmos. Terr. Phys., **48**, 777–785.
Wannberg, U.G., Wolf, I., Vanhainen, L.-G., Koskenniemi, K., Röttger, J., Postila, M., Markkanen, J., Jacobsen, R., Stenberg, A., Larsen, R., Eliassen, S., Heck, S. and Huuskonen, A. (1997): The EISCAT Svalbard Radar, a case study in modern incoherent scatter radar system design. Radio Sci., **32**, 2283–2307.
Weinstock, J. (1978): Vertical turbulent diffusion in a stably stratified fluid. J. Atmos. Sci., **35**, 1022–1027.

(Received October 8, 1999; Revised manuscript accepted December 7, 1999)